

---

# The time course of visual afterimages: Data and theory

---

Joshua Wede, Gregory Francis<sup>¶</sup>

Department of Psychological Sciences, Purdue University, 703 Third Street, West Lafayette, IN 47907-2004, USA; e-mail: gfrancis@psych.purdue.edu

Received 2 February 2005, in revised form 29 June 2005; published online 9 June 2006

---

**Abstract.** Sequential viewing of two orthogonally related patterns produces an afterimage of the first pattern (Vidyasagar et al, 1999 *Nature* **399** 422–423; Francis and Rothmayer, 2003 *Perception & Psychophysics* **65** 508–522). We investigated how the timing between the first stimulus (a vertical bar grating) and the second stimulus (a horizontal bar grating) affected the visibility of the afterimage (a perceived vertical grating). As the duration from offset of the first stimulus increased, reports of afterimages decreased. Holding fixed the total time from offset of the first stimulus and increasing the duration from offset of the second stimulus while decreasing the time between the first and second stimuli, caused a decrease in afterimage reports. We interpret this finding in terms of Grossberg's BCS–FCS (boundary contour system–feature contour system) theory. In this theory, the afterimage percept is the result of color complement after-responses in the FCS system interacting with orientation after-responses in the BCS system. The two types of after-responses interact at a stage of neural filling-in to produce the afterimage percept. As the duration between the stimuli increases, the color after-responses weaken so that visible filling-in is less likely to occur. A similar effect occurs for the orientation after-responses but at a faster time scale. Simulations of the model match the experimental data.

## 1 Introduction

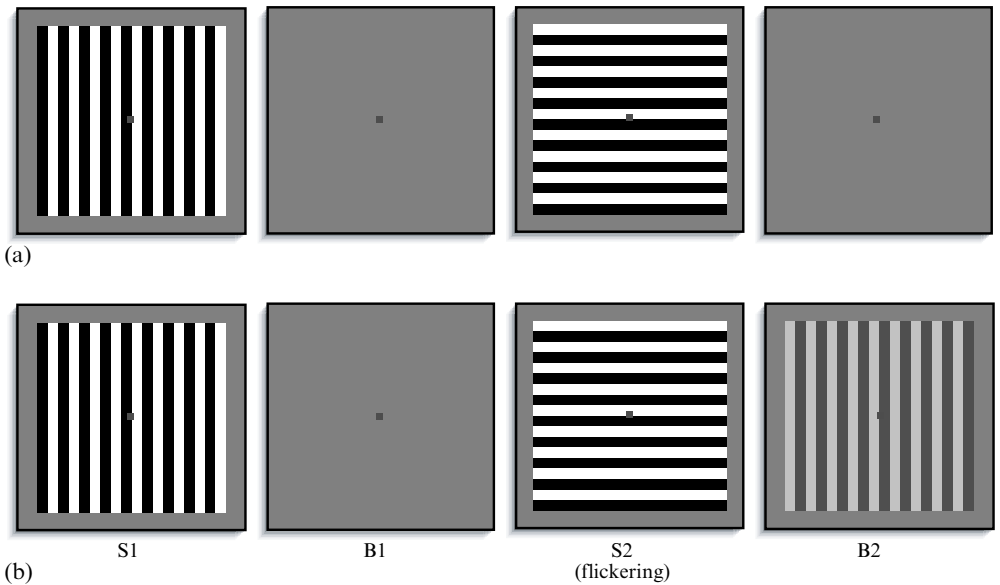
Francis and Rothmayer (2003) reported that sequential viewing of two orthogonally related patterns produces an afterimage percept related to the first pattern. They explained this afterimage using Grossberg's FACADE (1994) theory. Figure 1a shows a sequence of images that produce the afterimage (Francis and Rothmayer 2003). The first image (S1) consisted of black and white vertical bars on a gray background that was presented for 1 s. S1 was replaced by a blank gray screen (B1) for a duration of 1 s. B1 was then replaced by S2, which was made of a set of horizontal black and white bars that flickered with its achromatic color complement. Finally, the observer was shown another blank screen (B2) and at the end of this blank the observer was asked to report on any afterimages.

Figure 1b shows the percepts associated with the presentation of images. When observers were presented with a vertical or horizontal grating, they veridically saw those images. During B1 observers did not see any afterimages, but, during B2, observers reported seeing a vertical afterimage similar to S1. If S1 and S2 were of the same orientation, for example if both were horizontal gratings, observers reported few, if any, afterimages. Although the afterimage schematic in figure 1b looks more clearly defined than the actual percept, the afterimage was clearly observed.

These afterimages are probably the same type as the afterimages reported by Vidyasagar et al (1999). They showed a repeating sequence of radial arcs, blank screen, concentric circles, and a blank screen. Observers reported seeing an afterimage during the presentation of blank screens. Offset of the arcs produced an afterimage of concentric circles, while offset of concentric circles produced an afterimage of radial arcs.

These afterimages seem to be related to the orientation afterimages reported by MacKay (1957). In MacKay's experiments, observers stared at a pattern of radial arcs for 10 s.

<sup>¶</sup> Author to whom all correspondence should be addressed.



**Figure 1.** A schematic of (a) the stimuli and (b) percepts of the afterimage.

At offset of the stimulus, they reported seeing an aftereffect of concentric circles moving in circular orbits at right angles to the inducing stimulus. MacKay termed this after-response a complementary afterimage (CAI) to indicate that the shape of the afterimage is an orientation complement of the inducing image. A similar effect was also noted when the inducing stimulus was concentric circles. The complementary afterimage was seen to be radial arcs. Likewise, exposure to an oriented grating produced an aftereffect of streaming lines running orthogonal to the inducing grating.

Francis and Rothmayer (2003) distinguished the afterimage schematized in figure 1 from MacKay's by classifying the afterimages as modal or amodal percepts (Kanizsa 1979). Modal percepts include a phenomenological presence of color and brightness; amodal percepts do not. CAIs have shape and orientation, but seem to lack color or brightness, so they could be classified as amodal percepts. The afterimage studied by Francis and Rothmayer does have color and brightness, and should be classified as a modal percept. Francis and Rothmayer (2003) termed the afterimage schematized in figure 1 a modal CAI (MCAI).

Francis and Rothmayer (2003) and Francis and Schoonveld (2005) reported simulations of Grossberg's (1994) FACADE model that accounted for the appearance of MCAIs. In this theory, two separate pathways are used to compute visual information. Figure 2 shows a schematic of the major parts of the model. A boundary contour system (BCS) processes boundary or edge information, while a feature contour system (FCS) uses information from the BCS to allow diffusion of surface properties like color and brightness. The BCS detects oriented edges. The FCS uses the BCS information to determine where information spreads, leading to the final percept.

Embedded within the FACADE architecture are gated dipole circuits (Grossberg 1972). A gated dipole contains two pathways that compete as signals pass from lower to higher levels. A signal passing through one pathway inhibits a signal passing through the competing pathway. At offset of stimulation, a gated dipole circuit produces a reduction in cross-channel inhibition from the stimulated channel to the unstimulated channel. This reduction in inhibition leads to a rebound of activity in the unstimulated pathway. In the FACADE model, the properties of the gated dipole help to act as a reset signal to reduce persisting neural signals (Francis et al 1994). Gated dipoles have also

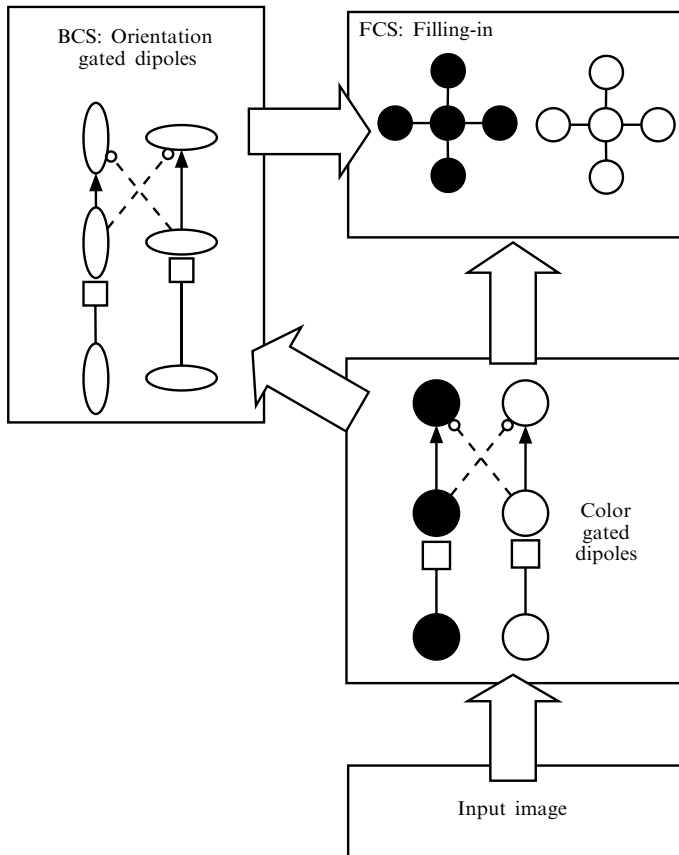


**Figure 2.** A schematic of the main components of FACADE theory. The input image feeds into a retinotopic representation of black and white, which compete in a gated dipole circuit. The gated dipole circuit produces complementary after-responses. The black-and-white information then feeds into edge detection in the boundary contour system (BCS), which also contains a gated dipole circuit whose after-responses code orthogonal orientations. The edges in the BCS guide the spread of black-and-white information in the filling-in stage to limit the spread of color and brightness information.

been used to account for effects such as motion perception (Kim and Francis 2000), and neurophysiological evidence has been found for gated dipoles (Abbot et al 1997).

There are separate gated dipole circuits in the FACADE architecture that code for color/brightness and orientation. Thus, at each pixel location there are two types of after-responses in the model. One codes the opposite color (only achromatic colors are considered in the current simulations) and the other codes the opposite orientation (vertical/horizontal in the current simulations). The combination of after-responses will produce a visible afterimage percept, only if the oriented boundary signals separate the color signals into distinct regions at the filling-in stage. The results of a simulation of these interactions in figure 3 show the development of MCAIs by presenting the different components of the model during a simulated trial.

Figure 3 contains information across model components, across space, and across time. Figures 3a, 3b, 3c, and 3d show the model behavior at different time periods during the course of a simulated experimental trial. All of the simulation images in figure 3 show the pattern of cell activities at the end of each stimulus duration. The color values in the image correspond to a difference in activity of the cells at that position (eg white minus black or vertical minus horizontal). The largest positive value

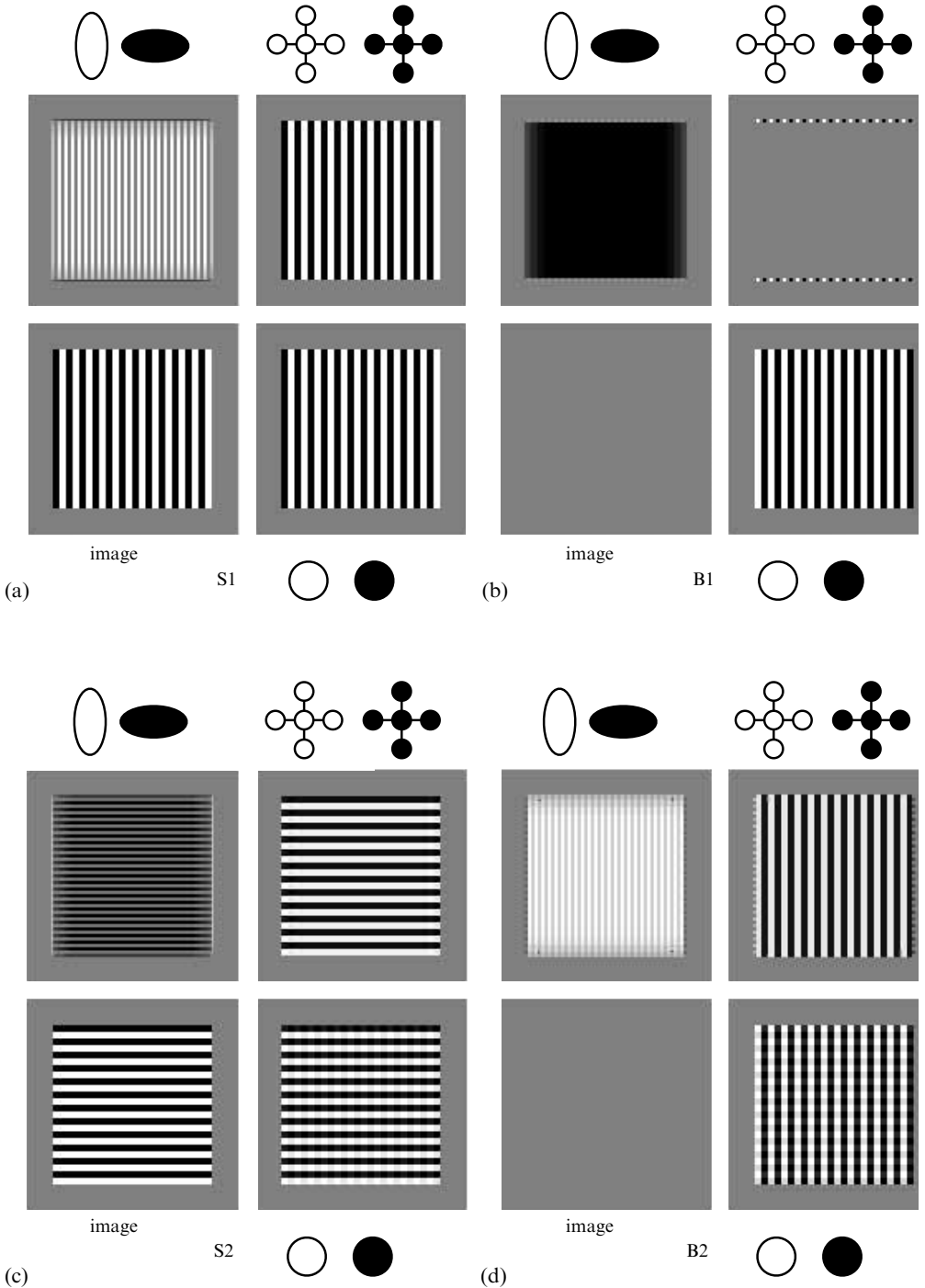


**Figure 3.** The results of a simulation of the model. See the main text for a description of each graph. (a) During presentation of a vertical bar grating (S1) there are strong vertical boundaries, and a vertical bar grating is present at the filling-in stage. (b) When the vertical bar grating is replaced by a blank screen (B1), there are color-complement after-responses and orientation after-responses. This combination of signals does not support an afterimage at the filling-in stage. (c) When the blank screen is replaced by a horizontal grating (S2), a horizontal percept is produced at the filling-in stage. (d) When the horizontal grating is replaced by another blank screen (B2), the MCAI afterimage is produced at the filling-in stage.

is set equal to white and the largest negative value is set equal to black. The value zero is always set to middle gray, and other positive and negative values are then scaled linearly to other gray values.

Within each subfigure, the four gray boxes correspond to different components of the model. A word or icon is associated with each gray box to indicate the corresponding model component in figure 2. The gray box on the bottom left, with the word 'image' below it, corresponds to the stimulus that was presented during this part of the trial. The gray box on the bottom right with the white and black circles displays the response from the color gated dipoles across a representation of visual space. The gray box on the upper left with the vertical and horizontal ovals displays the response from the orientation cells of the BCS across a representation of visual space. Black color at a pixel indicates a response from a horizontally tuned cell and white color at a pixel indicates a response from a vertically tuned cell. The gray box on the upper right corresponds to the activities across the filling-in stage.

The trial starts with the presentation of S1, a vertical black and white grating (figure 3a). The output of the color gated dipole shows the input from the vertical grating. The boundary signals are primarily vertical. The filling-in stage shows a black and white vertical grating, and thus a veridical percept.

Figure 3b shows the behavior of the model 1 s after offset of the vertical grating (end of B1). Two kinds of after-responses are generated. At the color gated dipole, the active color at each pixel is flipped so that what was black is now white and vice-versa. Likewise, at the orientation gated dipole, what was once vertical is now horizontal and vice-versa. In addition, boundary grouping in the BCS completes across the gaps between the vertically arranged horizontal orientations. As a result, there is a solid mass of dense horizontal signals (the black square). It should be emphasized that a black pixel indicates activity from a horizontally tuned cell; so the black square corresponds to a very dense array of activities among horizontally tuned cells.

When the vertically arranged color after-responses are joined with the horizontal orientation after-responses at the filling-in stage, no afterimage percept is produced. This is because the horizontal orientations allow color to flow left and right but not up and down. As a result, the black and white bars from the color signals spread over each other and cancel out. Except for a few edge effects, there is no visible after-image at the filling-in stage.

Figure 3c shows the behavior of the model at the end of the presentation of S2, a horizontal grating. As in the experiments of Francis and Rothmayer (2003), this horizontal grating flickered with its achromatic color complement and what is shown in figure 3c is the behavior of the model at the end of the last horizontal grating. The output of the color gated dipole shows predominately horizontally arranged black and white color signals, which are driven by the horizontal grating. However, faintly superimposed on the horizontal pattern are black and white vertical bars. (The faint vertical stripes may not be visible in the reproduction of the image.) These vertical stripes are color after-responses produced by the offset of the vertical grating. The orientation signals are predominately horizontal (black) because of two effects. First, the presentation of the horizontal image produces strong responses among horizontally tuned cells at the appropriate positions on the edges of the bars. The faint vertical stripes are too weak to produce any vertical boundaries. Second, the offset of the vertical grating continues to cause rebounds in the orientation gated dipoles that produce strong horizontal boundary responses. The filling-in stage shows a horizontal grating, which corresponds to a veridical percept.

Figure 3d shows the behavior of the model 1 s after the offset of the horizontal grating (end of B2). The input image is a blank gray background. The responses of the color gated dipoles are black and white that are mostly arranged vertically owing to

lingering after-responses from S1. In addition, there are relatively strong horizontally arranged color after-responses due to adaptation during S2. The orientation signals are primarily vertical, because offset of the horizontal bar grating produces after-responses among vertically tuned cells.

In this simulation (and all the simulations reported here), the gated dipole for color operates with a slower time constant than the gated dipole for orientation, which means the color after-responses fade more slowly than the orientation after-responses. Thus, the activities across the color gated dipoles are a combination of both inducing stimuli, but the activities across the orientation gated dipoles are almost entirely determined by the second stimulus.

The filling-in stage in figure 3d shows a vertical bar grating, which corresponds to the MCAI percept. The filling-in stage produces this pattern because the vertical boundary signals constrain the filling-in signals to spread only up and down, not left and right. Thus, the dark and light horizontal rows of inputs from the color gated dipole spread across each other and cancel out. On the other hand, the dark and light columns in the color gated dipole are kept separate and so support activity at the filling-in stage. The net effect is that the orientation after-responses force the filling-in stages to ‘pick out’ the vertical pattern in the outputs of the color gated dipoles.

## 2 Model predictions

If the FACADE explanation of MCAIs is correct, then the color after-responses must last longer than the orientation after-responses (Francis and Rothmayer 2003). Clearly, the color after-responses generated by the first stimulus must last long enough to contribute to the MCAI percept. Likewise, the orientation after-responses generated by the second stimulus must last long enough to contribute to the MCAI percept. At the same time, though, the orientation after-responses generated by the first stimulus must not last so long as to interfere with the orientation after-responses from the second stimulus.

In addition, the functional purpose of the orientation afterimages in the FACADE theory is to reset reverberating activity in cortical feedback circuits (Francis et al 1994). To meet such a need, the orientation after-responses need to operate on a faster time-scale than is necessary for the color after-responses.

Figure 4 shows the non-thresholded output of a color (white pathway) and an orientation (horizontal pathway) gated dipole circuit during the presentation of an MCAI-inducing stimulus sequence. S1 was a vertical black and white grating. The cells are at a position on the image that is black. So, the white output of the gated dipole

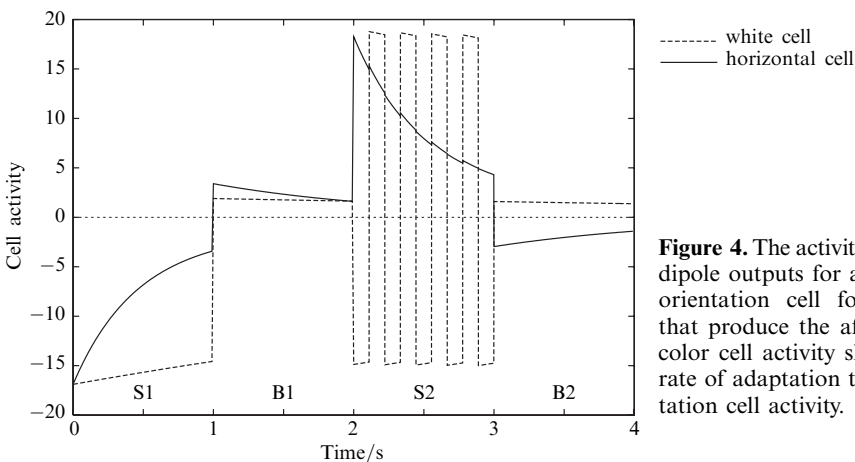


**Figure 4.** The activities of the gated dipole outputs for a color and an orientation cell for the stimuli that produce the afterimage. The color cell activity shows a slower rate of adaptation than the orientation cell activity.

at this position is inhibited; thus the activity of the white cell is negative. Likewise, because the orientation of the grating is vertical, the horizontally oriented cell is inhibited (negative). During the 1-s presentation of S1, the inhibition weakens as the habituating transmitter gate of the opposite channel becomes depleted. The change in inhibition is much faster and dramatic for the orientation circuit than for the color circuit.

After 1 s, the first frame is replaced by a blank gray screen (B1). During this time there are after-responses in both the white and horizontally tuned cells; both cell activities are positive. The after-responses fade during this time period, with the fading more dramatic for the orientation gated dipole than the color gated dipole. B1 is then replaced by a flickering horizontal grating (S2). The white cell tracks the flicker transitions, having positive activity when there is white input and negative activity when there is black input. In contrast, the horizontally tuned orientation cell has positive activity throughout this time because it is sensitive only to the orientation of the grating, regardless of the polarity of the grating bars. During this time, the response of the orientation-sensitive cell fades dramatically owing to the depletion of the neurotransmitter gate.

This fading sets up the orientation after-response that appears at 3 s, when the flickering grating is replaced by a gray blank (B2). The horizontally tuned cell shows a negative activity, which means that there is a positive activity in a vertically tuned cell at the same location. This after-response weakens as the neurotransmitter gate recovers.

In contrast, the white signal in the color gated dipole circuit still shows activity that reflects the after-responses generated by the first stimulus. Because the time scale of changes in the color gated dipole are much slower than in the orientation gated dipole, these after-responses can last for a substantial length of time. When the color and orientation after-responses are combined across space, they produce the MCAI percept at the filling-in stage of the model, as in figure 3.

Since the model suggests that an MCAI requires both the color after-responses of the first stimulus and the orientation after-responses of the second stimulus, the MCAI should fade away whenever either set of after-responses disappears. As figure 4 indicates, the orientation after-responses from S2 fade faster than the color after-responses from S1.

The different time courses of model color and orientation after-responses can be demonstrated by isolating each component. Figure 5a shows a measure of the model afterimage strength as a function of the duration between offset of S1 and the end of B2.

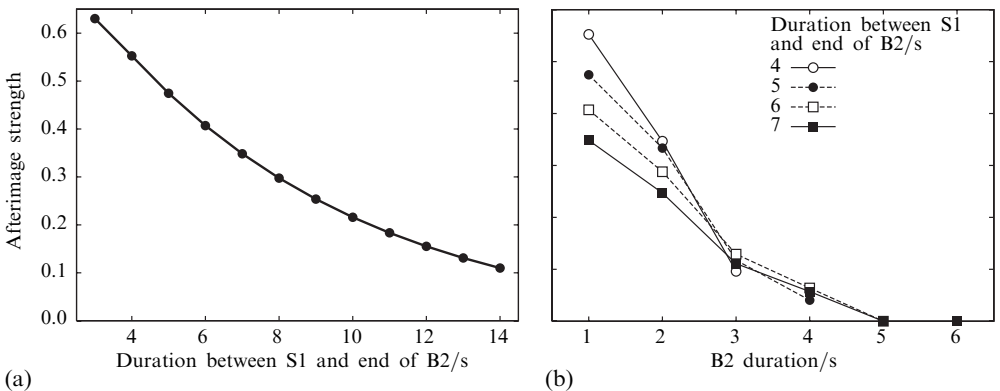


**Figure 5.** Model predictions. (a) Fixing the duration of S1, S2, and B2 and increasing the delay between the offset of S1 and the end of B2, by varying the duration of B1, should lead to a decrease in reports of the afterimage. (b) The model further predicts that for a fixed duration between S1 and the end of B2, increases in the duration of B2, with corresponding decreases in B1, should lead to a decrease in reports of the afterimage.

---

In these simulations the durations of S1, S2, and B2 were all held fixed at 1 s. As a result, the orientation after-responses generated by S2 should fade a constant amount during the fixed B2. Any changes in the afterimage strength must be due to the fading of color after-responses generated by S1.

With the current parameters, the model predicts that afterimage percepts should fade away after around 10–15 s. This is not a strong prediction of the model, though, because a different set of parameters could modify the quantitative values substantially. The main prediction is that reports of the afterimage should be less common as the delay between S1 and the end of B2 increases.

It is hardly surprising that an afterimage should fade away, but the prediction is more interesting when compared to the simulation data in figure 5b. For each curve in figure 5b, the total duration between S1 and the end of B2 is held fixed. Thus, the strength of the color after-responses generated by S1 should be fairly constant. Nevertheless, the model simulations predict substantial variation in afterimage strength as a function of B2 duration. As the duration of B2 increased (which means the duration of B1 decreased so that their sum was constant), the orientation after-responses generated by S2 faded. The fading of the orientation after-responses leads to substantial changes in the afterimage strength, even though the magnitudes of the color after-responses were nearly constant. With the current model parameters, this suggests that the orientation after-responses last for around 5 s, or only half as long as the color after-responses. This model prediction highlights that the MCAI requires two types of after-responses and that the two after-response types operate on different time scales.

Finally, the model predicts that the effect of total duration identified in figure 5a should be strongest for short durations of B2. At longer B2 durations, the model predicts a convergence of afterimage strength, regardless of the duration between S2 and the end of B2 (figure 5b). This is because at the short B2 durations, the difference in the strength of the afterimage is dependent on differences in the strength of the color after-responses. All of the orientation after-responses are strong enough to contribute to a strong afterimage if sufficient color after-responses are available. However, at longer B2 durations, the strength of the afterimage is determined by the availability of orientation after-responses, whose strengths are determined almost solely by the B2 duration.

There is a smaller effect that involves an interaction of the orientation and color after-responses. At longer B2 durations, there is a corresponding decrease in B1 duration. When S1 and S2 appear quickly after each other, the strength of the orientation after-response at offset of S2 can be weakened by the continued adaptation that developed during S1. As a result, for the shortest B1 durations, the model predicts a small increase of afterimage strength with increases in the duration between S1 and the end of B2. Figure 5b shows this reversal at B2 durations of 3 and 4 s. The following two experiments test these model predictions.

### **3 Experiment 1: Time course of color after-responses**

#### *3.1 Methods and procedures*

Figure 6 schematizes the stimuli used in each trial. Observers were instructed to stare at a red square in the center of the computer screen. A vertical grating (S1) was shown for 1 s, followed by a blank screen (B1), which varied in duration between trials. The blank screen was replaced by a second stimulus (S2), consisting of a horizontal bar grating that flickered with its achromatic color complement for a total of 1 s. Each of the two frames making up S2 was presented for 100 ms before being replaced by the other. The second stimulus was followed by a second blank screen (B2), shown for 1 s. At the end of the trial, a box filled with random dots was shown and the observer's task was to report any afterimage seen just before the random dots were shown.

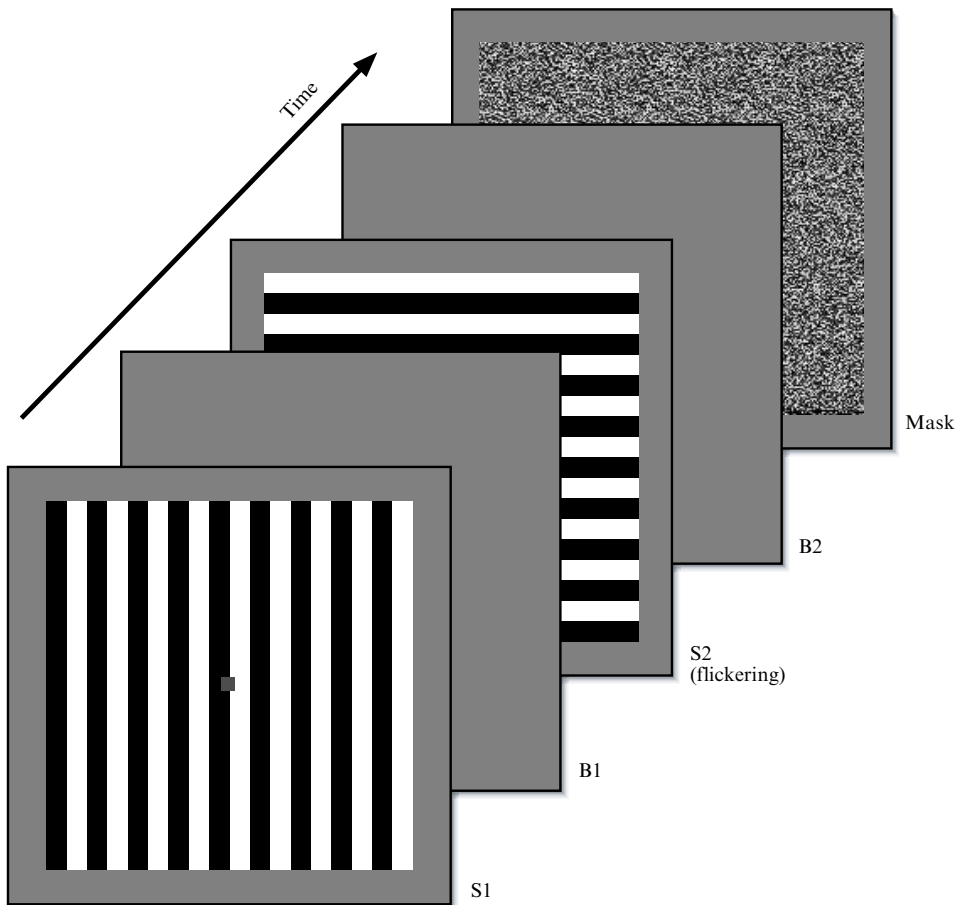


**Figure 6.** The sequence of frames during a trial of the experiments. The observer's task was to report on any seen afterimages just before the box of random dots appeared.

All stimuli were created and presented with MATLAB, with the Psychophysics Toolbox extensions (Brainard 1997; Pelli 1997), on a PC running Windows 2000 with a monitor that refreshed at 75 Hz.

The S1 and S2 gratings consisted of 10 black ( $0.16 \text{ cd m}^{-2}$ ) and 10 white ( $120 \text{ cd m}^{-2}$ ) equal-sized alternating bars. The height and width of the grating was 12.1 deg. The gratings were centered on the screen and presented on a gray ( $24 \text{ cd m}^{-2}$ ) background. A red square was placed in the middle of the grating as a fixation point for observers. S1 was always vertical and S2 was always horizontal. There were four conditions that varied the duration of B1 as 3, 6, 9, or 12 s. Since S2 and B2 each have a duration of 1 s, the duration between offset of S1 and the end of B2 was 5, 8, 11, and 14 s.

Seven naive observers from the experimental subject pool at Purdue University participated in return for course credit. Observers viewed the monitor from a distance of 52 cm, and his/her head was placed in a headrest to minimize movements. The observer was asked to keep eyes fixated on the red square in the middle of the screen.

After seeing all the stimuli, the observer indicated, by pressing a key, what type of afterimage he/she saw, if any. The observers were given three choices: "nothing", "vertical", and "horizontal", and were told to report what they saw at the moment right before the box of random dots appeared (the end of B2). They were instructed to report "nothing" only if they saw no afterimage at all. If they saw any afterimage, they were to choose whether it was best described as vertical or horizontal.

Each observer viewed the four conditions 12 times, for a total of 48 trials. Observers worked through the experiment at their own pace, with a key-press starting each trial. A minimum 20 s delay was introduced between trials to reduce across-trials effects. The experiment took approximately 30 min to complete.

### 3.2 Results

Results for experiment 1 are shown in figure 7a, in which the proportion of trials in which a vertical afterimage was reported is plotted as a function of the duration between offset of S1 and the end of B2. The vertical afterimage corresponds to an MCAI. Each proportion is combined across all observers and is based on 84 trials. Reports of horizontal afterimages were quite rare (1%, 2%, 1%, and 6% of the trials for the four durations, respectively); most reports were either of a vertical afterimage or of no afterimage at all.

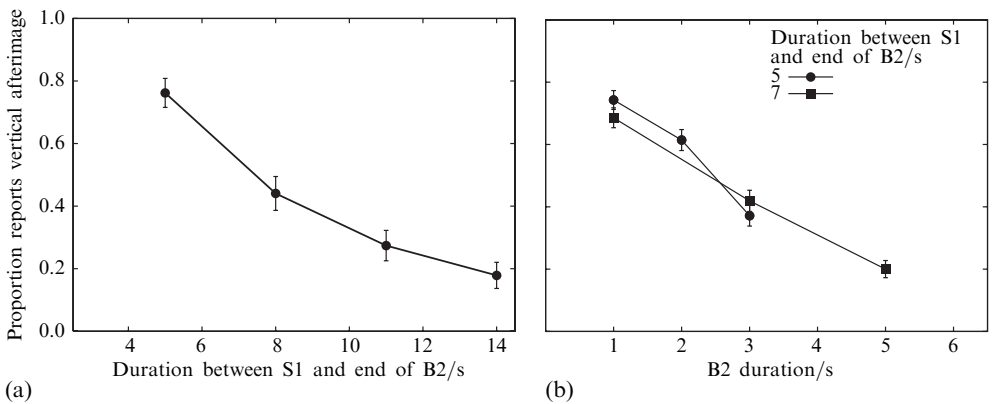


**Figure 7.** Data from experiments 1 and 2. An error bar corresponds to one standard error of proportion. (a) The data from experiment 1 show decreases in reports of the afterimage when B2 was fixed and B1 increased. (b) The data from experiment 2 show that when the sum of B1 and B2 durations was held fixed, afterimage reports decrease with larger B2 duration.

As the duration between S1 and the end of B2 increased from 5 to 14 s, the proportion of reports of afterimages decreased. An analysis of variance showed that the effect of the duration between S1 and the mask was significant ( $F_{3,18} = 16.68, p \leq 0.0001$ ).

### 3.3 Discussion

The results of experiment 1 agree with the model predictions. More generally, the results indicate that reports of an MCAI fade as the delay between S1 and the mask cue increases. Because B2 was held fixed to 1 s, the model predicts that the strength of the orientation after-responses from S2 should be constant, so the fading of the percept must be due to the fading of the color after-responses generated by S1. Thus, from the perspective of the model, the color after-responses must last at least 14 s on some trials.

## 4 Experiment 2: Time course of orientation after-responses

The method for experiment 2 was essentially the same as for experiment 1. The presentation of stimuli was the same as in experiment 1, except that the durations of B1 and B2 varied across conditions. Observers were shown S1 for 1 s, followed by B1 which varied in duration. Then S2 was shown for 1 s, followed by B2 which varied in duration. S1 and S2 were the same stimuli as those used in experiment 1.

The sum of B1 and B2 was fixed at either 4 s or 6 s. This means that the total duration between the offset of S1 and the end of B2 was either 5 or 7 s. For each total duration there were three combinations of B1/B2 durations. In the 5 s condition

the combinations were  $\frac{1}{3}$ ,  $\frac{2}{2}$ , and  $\frac{3}{1}$  s. In the 7 s condition, the B1/B2 durations were  $\frac{1}{5}$ ,  $\frac{3}{3}$ , and  $\frac{5}{1}$  s. Thirty observers from the experimental subject pool at Purdue University participated for course credit. Fifteen observers completed the 5 s total condition and the other fifteen completed the 7 s total condition. Each observer saw each combination of B1/B2 durations in his/her respective condition 14 times for a total of 42 trials.

#### 4.1 Results

The results for experiment 2 are shown in figure 7b, in which the proportion of times observers reported seeing a vertical afterimage is plotted for each combination of the B1/B2 times. Each proportion is based on 210 trials. Most observers never reported seeing a horizontal afterimage. (When the duration between S1 and the end of B2 equaled 5 s, the percentage of trials that observers reported seeing a horizontal afterimage was 4%, 3%, and 2% for each of the B2 durations, respectively. For the 7 s duration between S1 and the end of B2, the percentage of trials with a reported horizontal afterimage equaled 5%, 4%, and 1% for each of the B2 durations, respectively.) Separate curves in figure 7b show the results for the 5 and 7 s durations between offset of S1 and onset of the cue to report. For a fixed total duration, observers reported substantially fewer vertical afterimages as the B2 duration increased. This trend is significant for both the 5 s ( $F_{2,28} = 24.11$ ,  $p < 0.0001$ ) and 7 s ( $F_{2,28} = 14.67$ ,  $p < 0.0001$ ) conditions.

Although the data do suggest a bigger difference between the 5 and 7 s conditions for the shorter B2 durations than for the longer B2 durations, none of the differences are statistically significant. However, across all B2 durations, reports of an afterimage were less common for the 5 s condition ( $p = 0.58$ ) than for the 7 s condition ( $p = 0.43$ ). This difference is statistically significant ( $t = 5.01$ ,  $p < 0.0001$ ); and is generally consistent with the effects found in experiment 1.

#### 4.2 Discussion

As predicted by the model, the visibility of the afterimage is not solely a function of the time since offset of S1. Instead, even with the time since offset of S1 held constant, reports of the afterimage decreased as B2 duration increased. This suggests that the orientation after-responses generated by S2 fade faster than the color after-responses generated by S1 and that both types of after-responses are needed for the MCAI to be visible.

A more global perspective of the match between the model and the experimental data can be seen in figure 8, in which the proportion of reports of seeing an MCAI afterimage, for both experiments, is plotted against the afterimage strength predicted

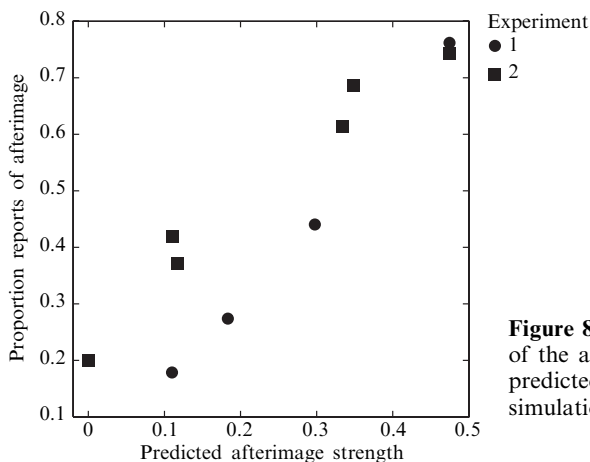


**Figure 8.** A scatterplot of proportion of reports of seeing the afterimage from the experiments and the predicted afterimage strength from the model simulations.

by the model. The data are in fairly good agreement with the model predictions. The correlation between the data and the model predictions is  $r = 0.92$ , which is statistically significant. The only notable deviation of the data from the model prediction is that the data for experiment 1 seem to be on one line (with  $r = 0.99$ ), while the data for experiment 2 seem to be on a close but different line (with  $r = 0.98$ ).

## 5 Conclusions

We analyzed the relative decay rates of color and orientation after-responses in the FACADE model. To account for the existence of the MCAI afterimage, Francis and Rothmayer (2003) predicted that the decay rate of orientation after-responses would be faster than the decay rate of color after-responses. We identified how to isolate the effect each type of after-response has on the strength of MCAI afterimages. The simulations and experimental data both agree with the predicted difference in decay rates.

Previous studies of afterimages are generally in agreement with this conclusion. Of course, it is difficult to compare results across studies because of differences in stimuli, exposure duration, and methods of measurement. Nevertheless, on a flickering background, color afterimages can last for nearly 5 min (Magnussen and Torjussen 1974), which suggests that the neural after-responses responsible for the afterimage percept must last at least that long. Without a flickering background, color afterimages often last for around 6 s (Kelly and Martinez-Uriegas 1993; Suzuki and Grabowecy 2003). In contrast, MacKay (1961) reported that orientation-based complementary afterimages seem to last only 1 or 2 s. There are so few studies of orientation afterimages that it is difficult to judge whether this is a reliable upper limit for their duration. Nevertheless, our results are consistent with the idea that the neural after-responses responsible for orientation aftereffects operate at a faster time scale than those responsible for color afterimages.

A precise neurophysiological basis of afterimages remains unclear, but it is certain that both retinal and cortical mechanisms are involved (see the discussion in Hofstoetter et al 2004). Many parts of the FACADE model that we used to predict and interpret the experimental data have been implemented in a neurophysiological model of visual cortex called LAMINART (eg Grossberg 2001; Grossberg and Williamson 2001; Grossberg and Yazdanbakhsh 2005; Raizada and Grossberg 2003). Future work on this model that identifies the sites of neural after-responses should help guide the exploration and interpretation of the neurophysiological basis of afterimages.

## References

- Abbot L F, Varela J A, Sen K, Nelson S B, 1997 "Synaptic depression and cortical gain control" *Science* **275** 220–224
- Brainard D H, 1997 "The Psychophysics Toolbox" *Spatial Vision* **10** 433–436
- Francis G, Grossberg S, Mingolla E, 1994 "Cortical dynamics of feature binding and reset: Control of visual persistence" *Vision Research* **34** 1089–1104
- Francis G, Rothmayer M, 2003 "Interactions of afterimages for orientation and color: Experimental data and model simulations" *Perception & Psychophysics* **65** 508–522
- Francis G, Schoonveld W, 2005 "Using afterimages for orientation and color to explore mechanisms of visual filling-in" *Perception & Psychophysics* **67** 383–397
- Grossberg S, 1972 "A neural theory of punishment and avoidance: II. Quantitative theory" *Mathematical Biosciences* **15** 253–285
- Grossberg S, 1994 "3-D vision and figure-ground separation by visual cortex" *Perception & Psychophysics* **55** 48–120
- Grossberg S, 2001 "Linking the laminar circuits of visual cortex to visual perception: Development, grouping, and attention" *Neuroscience and Biobehavioral Reviews* **25** 513–526
- Grossberg S, Mingolla E, Ross W D, 1997 "Visual brain and visual perception: How does the cortex do perceptual grouping?" *Trends in Neurosciences* **20** 106–111

- 
- Grossberg S, Williamson J R, 2001 “A neural model of how horizontal and interlaminar connections of visual cortex develop into adult circuits that carry out perceptual groupings and learning” *Cerebral Cortex* **11** 37–58
- Grossberg S, Yazdanbakhsh A, 2005 “Laminar cortical dynamics of 3D surface perception: Stratification, transparency, and neon color spreading” *Vision Research* **45** 1725–1743
- Hofstoetter C, Koch C, Kiper D C, 2004 “Motion-induced blindness does not affect the formation of negative afterimages” *Consciousness and Cognition* **13** 691–708
- Kanizsa G, 1979 *Organization in Vision. Essays on Gestalt Perception* (New York: Praeger)
- Kim H, Francis G, 2000 “Perceived motion in complementary afterimages: verification of a neural network theory” *Spatial Vision* **13** 67–86
- Kelly D H, Martinez-Uriegas E, 1993 “Measurements of chromatic and achromatic afterimages” *Journal of the Optical Society of America A* **10** 29–37
- MacKay D M, 1957 “Moving visual images produced by regular stationary patterns” *Nature* **180** 849–850
- MacKay D M, 1961 “Interactive processes in visual perception”, in *Sensory Communication* Ed. W A Rosenblith (Cambridge, MA: MIT Press) pp 339–355
- Magnussen S, Torjussen T, 1974 “Sustained visual afterimages” *Vision Research* **14** 743–744
- Pelli D G, 1997 “The VideoToolbox software for visual psychophysics: Transforming numbers into movies” *Spatial Vision* **10** 437–442
- Raizada R, Grossberg S, 2003 “Towards a theory of the laminar architecture of cerebral cortex: Computational clues from the visual system” *Cerebral Cortex* **13** 100–113
- Suzuki S, Grabowecky M, 2003 “Attention during adaptation weakens negative after-images” *Journal of Experimental Psychology: Human Perception and Performance* **29** 793–807
- Vidyasagar T R, Buzas P, Kisyarday Z F, Eysel U T, 1999 “Release from inhibition reveals the visual past” *Nature* **399** 422–423

## Appendix: Simulations

### A1 Image plane: Input image

Each pixel  $(i, j)$  had an input value  $I_{i,j}$ . All the images used intensities between  $-1$  (black) and  $+1$  (white), with 0 indicating middle gray. A 128 by 128 pixel plane was used in all simulated images. Each bar grating image was 96 by 96 pixels on a gray background. The thickness of each black or white bar was 4 pixels. The first (vertical) and second (horizontal) stimuli were presented for one simulated time unit (equivalent to 1 s) each. The second grating flickered (black and white values changed places) 9 times.

### A2 Color gated dipole

The  $I_{i,j}$  value at each pixel fed into a color grating dipole. Here black and white signals were sent through opponent channels and habituation of those channels occurred. The habituating gate for the white channel at pixel  $(i, j)$ ,  $g_{i,j}$ , obeyed the differential equation:

$$\frac{dg_{i,j}}{dt} = \{A - Bg_{i,j} - Cg_{i,j}([I_{i,j}]^+ + J)\}D. \quad (\text{A1})$$

The term  $A - Bg_{i,j}$  describes a process whereby the gate amount increases toward the value  $A/B$ . The last subtraction describes depletion of the gate by the presence of a tonic signal  $J$  and by a white signal,  $[I_{i,j}]^+$ , where the notation  $[ ]^+$  indicates that negative values are set to zero. Parameter  $D$  controls the overall rate of change of the equation.

The black opponent pathway had an identical type of equation with only the term  $[I_{i,j}]^+$  replaced by  $[-I_{i,j}]^+$ , so that only black signals passed through the gate. In the following equations the habituating gate for the black pathway is labeled as  $G_{i,j}$ . Each simulation trial started with an initial value of gates that corresponded to an equilibrium value of the gates with no outside input:

$$g_{i,j}(0) = G_{i,j}(0) = \frac{A}{B + CJ}. \quad (\text{A2})$$

The parameters were set as  $A = 1$ ,  $B = 0.9$ ,  $C = 1$ ,  $D = 0.025$ , and  $J = 5$ .

The white output of the color gated dipole was then computed by weighting the net input into the white channel by its gate and then subtracting the resulting value by the weighted black input. The resulting difference was thresholded and then scaled. The white output,  $w_{i,j}$ , was computed as:

$$w_{i,j} = E\{([I_{i,j}]^+ + J)g_{i,j} - ([-I_{i,j}]^+ + J)G_{i,j} - F\}^+. \quad (\text{A3})$$

Here,  $F = 0.0004$  is a threshold, the term to its left is the inhibitory input from the black channel, and the next term to the left is the excitatory input from the lower levels of the white channel. The difference is rectified so that negative values are set to zero and then scaled by the multiplying term  $E = 100$ . The black output of the gated dipole,  $b_{i,j}$ , had a similar equation, with only the middle and left terms trading excitatory and inhibitory roles. The value  $w_{i,j} - b_{i,j}$  was plotted in the simulation images of figure 3 (bottom right frame).

### A3 Boundary contour system

#### A3.1 Edge detection and orientation gated dipole

The  $w_{i,j}$  and  $b_{i,j}$  values were sent to the BCS for edge detection. At each pixel, detectors were sensitive for an activation pattern that signaled either a vertical or horizontal edge. For computational simplicity detectors were used that just looked for a change in luminance intensity in a vertical or horizontal direction. The absolute value

of this change was taken as the response of the detector. A boundary cell at position  $(i, j)$  tuned to a vertical edge had an activity

$$y_{i,j} = [|w_{i,j} - w_{i-1,j}| + |w_{i,j} - w_{i+1,j}| + |b_{i,j} - b_{i-1,j}| + |b_{i,j} - b_{i+1,j}| - K]^+ . \quad (\text{A4})$$

This receptive field looks to the left and right of the edge location for any discontinuities among the white or black representations of color. The term  $K = 8$  indicates a threshold. Any values below  $K$  were set to zero. A similar value,  $Y_{i,j}$ , was computed for the horizontally tuned boundary cells.

The equations for the BCS oriented gated dipole had the same form as those used for the color gated dipole. The only differences from the equations of the color gated dipole are that in the BCS version of equations (A2) and (A4),  $[I_{i,j}]^+$  is replaced by  $y_{i,j}$  (vertical),  $[-I_{i,j}]^+$  is replaced by  $Y_{i,j}$  (horizontal),  $B = 5$ ,  $D = 0.05$ ,  $J = 10$ ,  $E = 10$ , and  $F = 8$ . The relevant equations are:

$$\frac{dg_{i,j}}{dt} = [A - Bg_{i,j} - Cg_{i,j}(y_{i,j} + J)]D \quad (\text{A5})$$

and

$$x_{i,j} = E[(y_{i,j} + J)g_{i,j} - (Y_{i,j} + J)G_{i,j} - F]^+ . \quad (\text{A6})$$

Here,  $x_{i,j}$  refers to the output of the orientation gated dipole for a vertically tuned cell. Since the outputs of the color gated dipole feed into the orientation detectors, which in turn feed into the habituated gates for the orientation gated dipole, the differential equations for both sets of the habituated gates were solved simultaneously. The equations were solved by Euler's method with a step size of 0.01 time units.

### A3.2 Boundary grouping

Grouping of BCS signals is supported by model bipole cells. Each vertically tuned bipole cell received excitation from vertically tuned gated dipole output cells and received inhibition from horizontally tuned gated dipole output cells. A vertical bipole cell had two sides (Up and Down) that separately combined excitatory and inhibitory inputs from the lower level. Each side combined information from a column of locations above (Up) or below (Down) the location of the bipole cell. For a vertical bipole cell at position  $(i, j)$ , the intermediate terms are:

$$\text{Up}_{i,j} = \left[ \sum_{k=0}^M (x_{i,j-k} - X_{i,j-k}) \right]^+ \quad (\text{A7})$$

and

$$\text{Down}_{i,j} = \left[ \sum_{k=0}^M (x_{i,j+k} - X_{i,j+k}) \right]^+ , \quad (\text{A8})$$

where  $x_{i,j}$  and  $X_{i,j}$  refer to the output of the orientation gated dipole for vertically and horizontally tuned cells, respectively.  $M = 10$  sets the reach of a bipole cell lobe. A bipole cell has a positive activity if both of the intermediate terms are non-zero, or the bottom-up edge information at the bipole cell's pixel location is non-zero and one of the intermediate terms is also non-zero. Thus, the activity of the vertical bipole cell at pixel  $(i, j)$  is:

$$B_{i,j} = \max(\text{Up}_{i,j} \text{Down}_{i,j}; x_{i,j} \text{Up}_{i,j}; x_{i,j} \text{Down}_{i,j}) . \quad (\text{A9})$$

This allows bipole cells to respond as if they interpolate, but do not extrapolate, bottom-up contour information. A vertical bipole cell will also respond if an oriented edge is present at the location of the bipole cell and a vertical oriented edge is above

or below the location of the bipole cell. Similar equations exist for each horizontally tuned bipole cell, which received excitatory input from other horizontally tuned cells and inhibitory input from vertically tuned cells.

To avoid proliferation of bipole cell responses, a second competition between orientations at each pixel was included. This competition was winner-take-all, so that the orientation bipole cell with the largest value received a value of twice the average inputs feeding into the cell ( $Up_{i,j} + Down_{i,j}$ ), while the other orientation bipole cell was given a value of 0. The set of values of each orientation at each pixel location was taken as the 'output' of the BCS. A pixel was said to have a vertical boundary if the vertically tuned cell won the competition here. A more elaborate version of this type of competition can be found in Grossberg et al (1997). The outputs of the bipole boundary signals are referred to as  $V_{i,j}$  and  $H_{i,j}$  for vertical and horizontal signals, respectively.

#### A4 Brightness filling-in

Filling-in of brightness information used the method described by Francis and Rothmayer (2003). Each fully connected region of the image was identified, and the brightness value of each pixel in that region,  $S_{i,j}$ , was set equal to the average of the  $w_{i,j} - b_{i,j}$  inputs of the region.

The strength of the filled-in afterimage (if any) was measured as the average absolute value of  $S_{i,j}$  across the image plane at the moment of the cue to report.

The strength of the  $w_{i,j} - b_{i,j}$  inputs to the filling-in stage is determined entirely by the relative timings of the stimuli and the delay before the cue to report. At the same time, the separation of black and white parts of the filling-in stage is determined by the absolute strength of the boundary signals. Whenever the boundaries are strong enough to support separate regions for filling-in, the strength of the afterimage is a constant value. Likewise, whenever the boundaries are too weak to support separate regions for filling-in, the afterimage strength goes to zero. If the simulations were run this way, the curves in figure 5b would be step functions rather than gradually decreasing.

Of course, if the model exists in the brain, it will not be purely deterministic. There would be various stages of noise that would add and subtract to the boundary and brightness values. Rather than add noise at each pixel location, which would dramatically increase simulation time, we introduced a variable threshold to the BCS boundaries. The boundary values that were used to identify separate regions in the filling-in stage were

$$[V_{i,j} - T]^+ \quad (\text{A10})$$

and

$$[H_{i,j} - T]^+ \quad (\text{A11})$$

for vertical and horizontal signals, respectively. The value of the threshold parameter  $T$  was varied systematically from 0.1 to 1.1 in steps of 0.2. For each threshold value, the afterimage strength after filling-in was measured and the average afterimage strength for all threshold values was computed. The average afterimage strength is reported in figure 5.